

# SPATIAL RESOLUTION WITH TIME-AND-POLARIZATION-RESOLVED ACOUSTIC MICROSCOPY

D. Xiang\* , N. N. Hsu, S. E. Fick and G. V. Blessing

Automated Production Technology Division  
National Institute of Standards and Technology  
Gaithersburg, MD 20899

## INTRODUCTION

Spatial resolution is an important factor in ultrasonic materials characterization. Scanning acoustic microscopy [1-2] has proved to be a useful tool for materials evaluation with micrometer-scale spatial resolution. Point-focus-beam (PFB) acoustic microscopy has high spatial resolution and is often used to produce images as well as to probe material inhomogeneity. However, a disadvantage of the PFB technique lies in its insensitivity to material anisotropy. In contrast, line-focus-beam (LFB) acoustic microscopy can provide a directional ultrasonic velocity measurement and is employed for characterization of anisotropic materials [3-5]. But the LFB technique, with its unidirectional spatial resolution, is generally incapable of producing images, and is therefore disadvantageous for probing inhomogeneous materials. In response to this need, a variety of lens designs [6-9] in acoustic microscopy have been proposed for measuring materials, which are both inhomogeneous and anisotropic.

Materials characterization with macroscopic (millimeter) spatial resolution can be achieved by time-and-polarization-resolved acoustic microscopy [10-11] utilizing a specially designed large aperture, low frequency, lensless, cylindrical polyvinylidene fluoride (PVDF) transducer [12] that is used in conjunction with conventional pulse-echo ultrasonic instrumentation. Macroscopic spatial resolution offers obvious economies in the extraction of engineering design data for materials such as composites.

Our purpose is to explore adjustment of the lateral spatial resolution of cylindrical PVDF transducers by simply changing the axial width of the active element, while keeping the thickness and circumferential length fixed. We use the radiated acoustic field pattern as an indicator of spatial resolution. Experimental results are given which verify that lateral spatial resolution can be improved. This facilitates inner-defect imaging and fiber-orientation-dependent leaky wave measurements on unidirectional composites.

---

\* NIST Guest Worker from the Johns Hopkins University, Baltimore, MD 21218

## TRANSDUCERS

Two prototype cylindrical PVDF transducers are compared in this paper. The first transducer uses a commercial flexible PVDF film (28  $\mu\text{m}$  thick with an effective area 12 mm x 30 mm) as the active element and tungsten-loaded epoxy as the backing material. The PVDF film constitutes the cylindrical front surface of the transducer. The rectangular aperture is 28.3 mm by 12 mm. The focal length of this transducer is 25.4 mm. Its center frequency is approximately 10 MHz, and its -3 dB bandwidth ( focal-point echo amplitude, shock excitation ) is 6 MHz. More details about the design, construction and application of this transducer can be found in a previous paper [12].

The second prototype transducer has the same configuration, except that the width of the active element is reduced from 12 mm to 0.5 mm (about three times the 10 MHz wavelength in water). To illustrate the beam profile measurements, we introduce the orthogonal coordinates as shown in Fig. 1, where the X and Y axes lie in the focal plane with the Y axis along the cylindrical axis, and the Z axis bisecting the focal line. The beam profiles in the X-Z and Y-Z planes can be used to depict the radiated acoustic fields.

### PLANAR SCANNING SETUP

A schematic of the experimental setup is shown in Fig. 2. The radiated acoustic fields in water were measured by planar scanning using a membrane hydrophone with a circular active element 0.4 mm in diameter. The PVDF membrane hydrophone has its acoustic impedance closely matched to that of water, and possesses a flat frequency response beyond the bandwidth of the transducers tested as shown in Fig. 3 (adapted from the manufacture's calibration data). A conventional pulser-receiver operated in through-transmission mode establishes the 180 volt (peak to peak) spike waveform applied to the transducer, and also provides 20 dB of amplification for the hydrophone signal. The amplified signal is captured using an 8-bit digital oscilloscope at a digitization rate of 250 megasamples per second. A desktop personal computer stores the peak-to-peak amplitude of the hydrophone signal for each point in the scanned plane and controls the mechanical scanning system (not shown in Fig. 2) used to move the hydrophone.

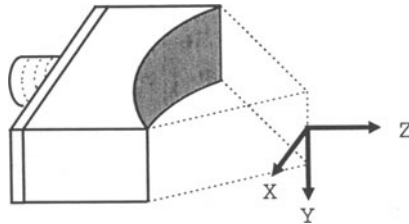


Fig. 1. Orthogonal coordinates for illustrating beam profiles of a cylindrical transducer.

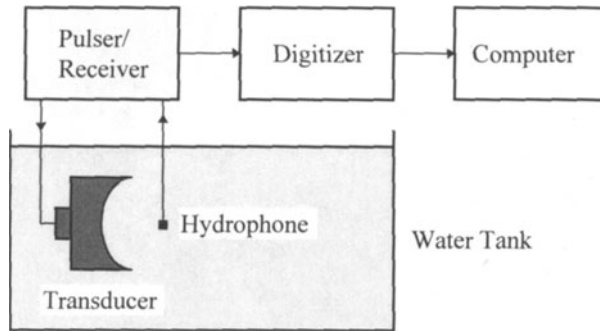


Fig. 2. Schematic of planar scanning setup.

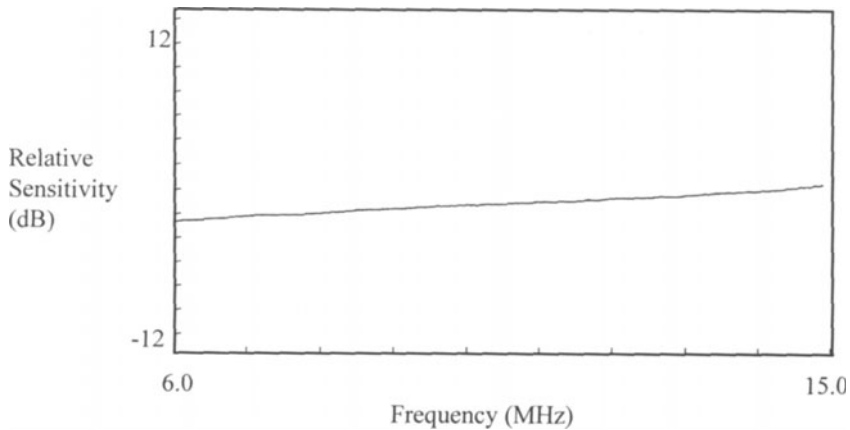


Fig. 3. Frequency response of the membrane hydrophone.

## BEAM PROFILES

Beam profile measurements were made in the focal region of the transducers, because this region is the most often used with cylindrical transducers. Beam profiles for the transducer with 12 mm element width are shown in Fig. 4 (X-Z plane) and Fig. 5 (Y-Z plane). The step interval is 0.5 mm. The focal plane is at  $Z = 0.0$  mm, and positive values of  $Z$  correspond to locations beyond the focal plane. Minus  $Z$  values are inside the focal region. The center of the transducer surface is located at  $Z = -25.4$  mm (not shown in Figs. 4 and 5). Sharp focusing in the X-Z plane is evident in Fig. 4. The beam profile in Fig. 5 shows that the received amplitude inside the focal region changes monotonically along the  $Z$  axis, and reaches its maximum at 0.0 mm. Furthermore, Fig. 5 confirms the expectation that the focus of a line-focus transducer will have a width related to the width of the active element of the transducer. By measuring the distance between the -3 dB (0.707 of the peak amplitude) points in the amplitude plots to indicate the spatial resolution [13], the dimensions of the focal spot in the X, Y and Z directions are found to be 0.3 mm, 10.6 mm and 5.6 mm respectively.

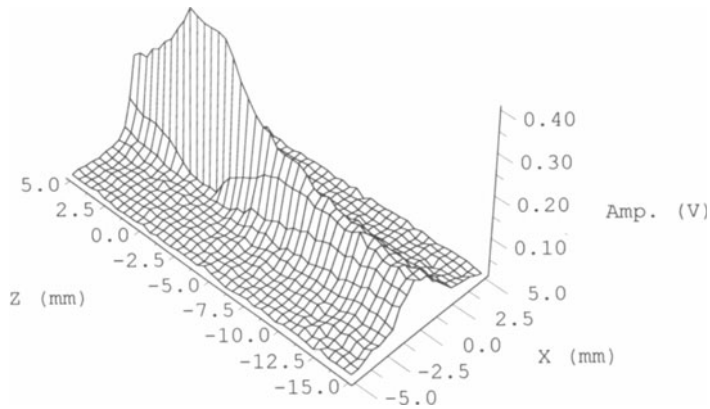


Fig. 4. Beam profile in X-Z plane of 12-mm-wide transducer.

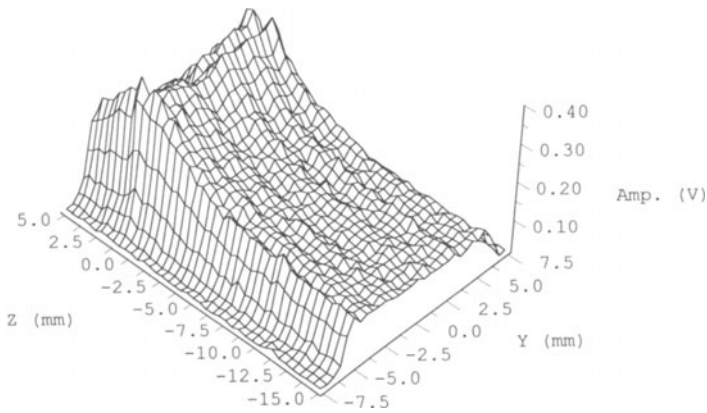


Fig. 5. Beam profile in Y-Z plane of 12-mm-wide transducer.

Beam profiles for the transducer with 0.5 mm element width are shown in Fig. 6 (X-Z plane) and Fig. 7 (Y-Z plane). The step interval is 0.2 mm. Sharp focusing in the X-Z plane is also evident in Fig. 6. By comparing Figs. 5 and 7, one can see that the narrower transducer produces a narrower focal width in the direction of the Y axis. By measuring the distance between -3 dB points in the amplitude plots, the dimensions of the focal spot in the X, Y and Z directions are found to be 0.3 mm, 2.2 mm and 6.4 mm respectively.

To allow comparison of the Y-axis focal-plane beamwidths of the two transducers, their respective amplitude profiles are shown in Fig. 8. As expected, the narrower transducer has a narrower lobe of lower amplitude. This means that, used as a receiver, the narrower transducer would have greater lateral spatial resolution, but at a cost of lower sensitivity.

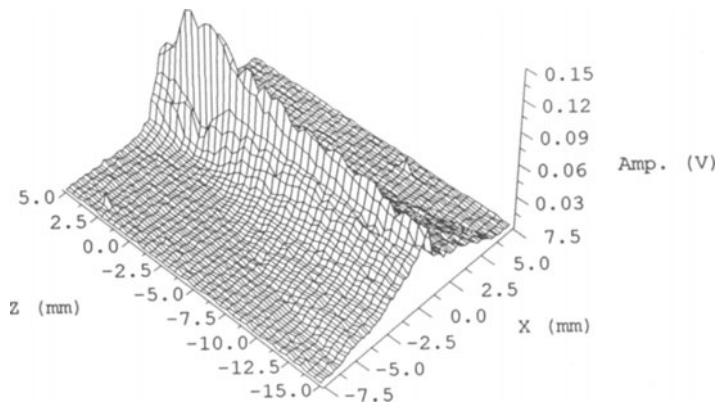


Fig. 6. Beam profile in X-Z plane of 0.5-mm-wide transducer.

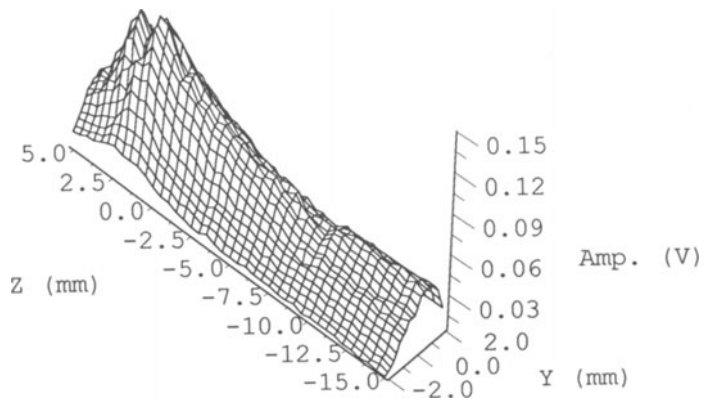


Fig. 7. Beam profile in Y-Z plane of 0.5-mm-wide transducer.

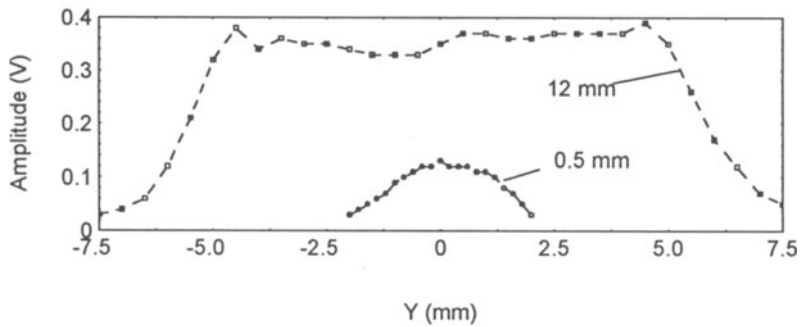


Fig. 8. Comparison of amplitude profiles in Y direction between 12 mm and 0.5 mm wide transducers.

## COMPOSITE MEASUREMENTS

Unidirectional carbon-fiber/epoxy composite, possessing a layered structure and anisotropic properties, is a material useful for a variety of purposes. One way to evaluate this material employs leaky waves launched and received by a pair of inclined transducers immersed in water [14]. Since our cylindrical PVDF transducers are suitable for launching and detecting leaky waves [10-12], the narrow transducer should also be useful for detecting fiber-orientation-dependent leaky waves on a unidirectional composite sample. We tested this assumption by rotating the transducer 360 degrees about its Z axis at a fixed defocus distance from the surface of such a sample. A gray-scale plot of the results is shown in Fig. 9, where 0 degrees is the direction of fiber orientation. The white band at the left (about 0.25  $\mu$ s) in the graph is the specular reflection from the surface. The wavy feature at its right, beyond 0.5  $\mu$ s, is attributable to leaky waves. Viewed from top to bottom, a 180-degree symmetry for the orientational dependence of the leaky waves is revealed. This symmetry is the result of the dependence of the leaky wave velocity in a unidirectional composite upon the angle between the axes of wave propagation and the fiber orientation. We note that this pattern is consistent with results obtained by Wolfe et al. [15] using a pair of focused transducers.

An image of another section of the unidirectional composite material is shown in Fig. 10. A blind hole 2 mm in diameter and 1 mm deep was made on one side of the 5 mm thick plate specimen. A planar scan was done from the unmarred side of the sample with the focal plane of the transducer set to coincide with the surface through which the hole passes. The scanned area in the X-Y plane is 10 mm by 10 mm, with 0.1 mm between pixels. Range gating of data for a single focal distance allows extraction of features for arbitrarily chosen planes within the specimen. Two such data ranges are shown in Fig. 10. The banded pattern at the top of the 3D plot, which corresponds to the top surface of the specimen, clearly shows the fiber orientation (along the black lines). The hole on the bottom surface of the specimen is clearly visible in the image.

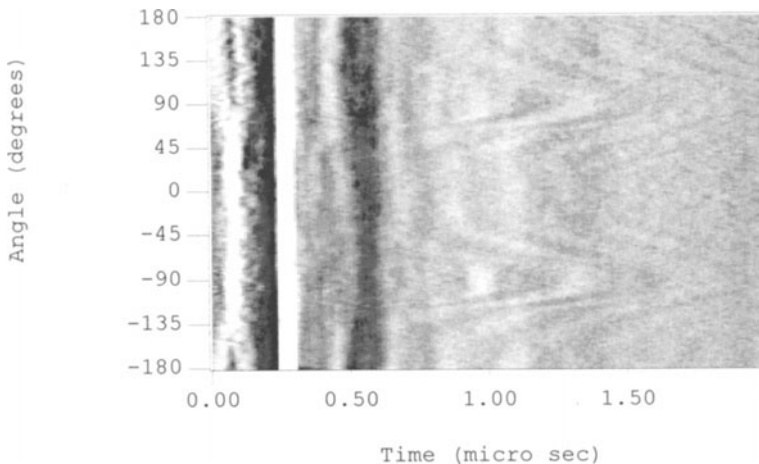


Fig. 9. Rotational scan of unidirectional composite using the 0.5-mm-wide transducer.

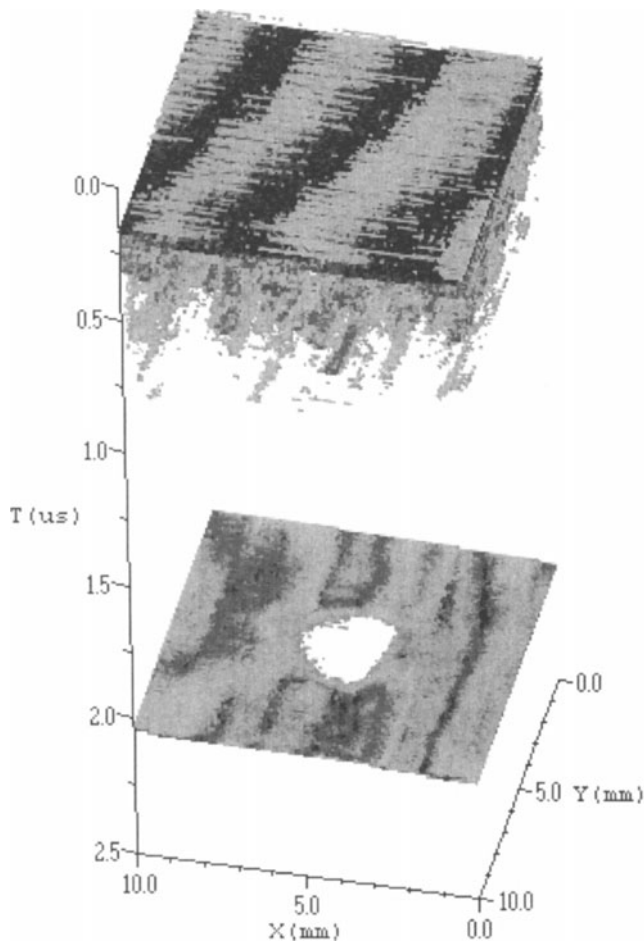


Fig. 10. Acoustic images of fiber orientation in the top surface and an artificial hole in the bottom surface of a unidirectional plate scanned by the 0.5-mm-wide transducer.

## CONCLUSION

Planar scanning with a membrane hydrophone has been used to determine beam profiles of cylindrical PVDF transducers developed for time-and-polarization-resolved acoustic microscopy. The radiated field patterns and focal spots of two cylindrical transducers of identical radius but different (0.5 mm vs. 12 mm) widths have been determined. The beam patterns confirm that reduction of the element width significantly decreased the transmitted beamwidth and increased lateral spatial resolution. Using the narrower transducer on a unidirectional composite sample, images of orientation-dependent leaky waves and an inner-defect have been obtained.

## ACKNOWLEDGEMENTS

The authors would like to thank Mr. Eric Su, a summer student from the Physics department at Cornell University, for programming the scanning and data acquisition system.

## REFERENCES

1. G. A. D. Briggs, *Acoustic Microscopy* (Clarendon Press, Oxford, 1992).
2. K. K. Liang, G. S. Kino and B. T. Khuri-Yakub, *IEEE Trans. Sonics and Ultras.*, SU-32, 213-224 (1985).
3. J. Kushibiki and N. Chubachi, *IEEE Trans. Sonics and Ultras.*, SU-32, 189-212 (1985).
4. J. O. Kim and J. D. Achenbach, *Thin Solid Films*, 214, 25-34 (1992).
5. C. Lee, J. O. Kim and J. D. Achenbach, *Ultrasonics*, 32, 359-365 (1994).
6. A. Atalar, *IEEE Trans. UFFC*, 36, 264-273 (1989).
7. D. A. Davids and H. L. Bertoni, *IEEE Ultrason. Symp.*, 735-740 (1986).
8. B. T. Khuri-Yakub and C-H. Chou, *IEEE Ultrason. Symp.*, 741-744 (1986).
9. T. Sannomiya, J. Kushibiki, N. Chubachi, K. Matsuno, R. Suganuma and Y. Shinozaki, *IEEE Ultrason. Symp.*, 731-734 (1992).
10. N. N. Hsu, D. Xiang and G. V. Blessing, *IEEE Ultrason. Symp.*, 867-871 (1995).
11. D. Xiang, N. N. Hsu and G. V. Blessing, *Rev. Prog. QNDE.*, 15, 1431-1438 (1996)
12. D. Xiang, N. N. Hsu and G. V. Blessing, *Ultrasonics*, 34, 641-647 (1996).
13. G. S. Kino, *Scanned Image Microscopy* (London: Academic, 1980).
14. D. E. Chimenti and R. W. Martin, *Ultrasonics*, 29, 13-21 (1991).
15. J. P. Wolfe and R. E. Vines, *IEEE Ultrason. Symp.*, 607-614 (1996).